THE JOURNAL OF BIOLOGICAL CHEMISTRY VOL. 285, NO. 48, pp. 37619–37629, November 26, 2010

Dual Modes of Interaction between XRCC4 and Polynucleotide Kinase/Phosphatase

IMPLICATIONS FOR NONHOMOLOGOUS END JOINING[*] [S]

Received for publication, August 24, 2009, and in revised form, August 23, 2010 Published, JBC Papers in Press, September 17, 2010, DOI 10.1074/jbc.M109.058719

Rajam S. Mani[‡], Yaping Yu[§], Shujuan Fang[§], Meiling Lu[‡], Mesfin Fanta[‡], Angela E. Zolner[§], Nasser Tahbaz[‡], Dale A. Ramsden[¶], David W. Litchfield[‖], Susan P. Lees-Miller[§1], and Michael Weinfeld[‡2]

From the [‡]Department of Oncology, University of Alberta, and the Cross Cancer Institute, Edmonton, Alberta T6G 1Z2, Canada, the [§]Department of Biochemistry and Molecular Biology and The Southern Alberta Cancer Research Institute, University of Calgary, Calgary, Alberta T2N 4N1, Canada, the [¶]Lineberger Comprehensive Cancer Center, Department of Biochemistry and Biophysics, University of North Carolina at Chapel Hill, Chapel Hill, North Carolina 27599, and the [‖]Department of Biochemistry, Schulich School of Medicine and Dentistry, University of Western Ontario, London, Ontario N6A 5C1, Canada

XRCC4 plays a crucial role in the nonhomologous end joining (NHEJ) pathway of DNA double-strand break repair acting as a scaffold protein that recruits other NHEJ proteins to double-strand breaks. Phosphorylation of XRCC4 by protein kinase CK2 promotes a high affinity interaction with the forkhead-associated domain of the end-processing enzyme polynucleotide kinase/phosphatase (PNKP). Here we reveal that unphosphorylated XRCC4 also interacts with PNKP through a lower affinity interaction site within the catalytic domain and that this interaction stimulates the turnover of PNKP. Unexpectedly, CK2-phosphorylated XRCC4 inhibited PNKP activity. Moreover, the XRCC4·DNA ligase IV complex also stimulated PNKP enzyme turnover, and this effect was independent of the phosphorylation of XRCC4 at threonine 233. Our results reveal that CK2-mediated phosphorylation of XRCC4 can have different effects on PNKP activity, with implications for the roles of XRCC4 and PNKP in NHEJ.

Efficient repair of DNA double-strand breaks (DSBs)[3] is critical for the maintenance of genome stability. In mammalian cells, nonhomologous end joining (NHEJ) is the major pathway that repairs these DSBs (1, 2). Although many of the individual components involved in the NHEJ repair pathway are well established, the dynamics of the repair pathway remains poorly understood. One approach to achieving a better understanding of the step-by-step choreography of each enzymatic process, including the nature of the binding of repair proteins to their DNA substrates and to each other, is to use a detailed quantitative approach in which specific protein-protein and protein-DNA interactions are not just identified qualitatively but are accurately quantified, giving an estimation of their respective affinities.

XRCC4 is regarded as a scaffold protein that recruits other proteins to DSBs (1). Of note, XRCC4 interacts with and catalytically stimulates the activity of DNA ligase IV (3, 4) to carry out the final step in the NHEJ pathway, joining the DNA ends (5). More recently, XRCC4 has been shown to interact with polynucleotide kinase/phosphatase (PNKP) (6, 7), a bifunctional enzyme that phosphorylates 5′-OH termini and dephosphorylates 3′-phosphate termini (8–11), thereby providing the correct chemical end groups required for DNA ligation by DNA ligase IV. Because XRCC4 is an efficient substrate for DNA-PK *in vitro* (12, 13), most studies have focused on the impact of DNA-PK-mediated phosphorylation on XRCC4 function (3, 14). However, phosphorylation of XRCC4 by DNA-PK cannot account for all of its functions. For instance, DNA-PK-dependent phosphorylation of XRCC4 does not appear to play a role in mediating resistance to ionizing radiation or V(D)J recombination (3, 14). On the other hand, phosphorylation by protein kinase CK2 mediates the interaction of XRCC4 with the forkhead-associated (FHA) domain of PNKP and thereby stimulates DNA ligation (7). An examination of the crystal structure of a short XRCC4 phospho-peptide bound to the FHA domain of PNKP indicated that this binding stems from electrostatic interaction of the CK2 phosphorylated residue (Thr-233) of XRCC4 and positively charged residues in the FHA domain of PNKP, particularly Arg-35 (15).

Given the central role of the XRCC4 protein in NHEJ, we initiated this study to understand the mode of interaction between XRCC4 and PNKP with a special emphasis on the role of XRCC4 phosphorylation by CK2. We have identified a novel, phosphorylation-independent interaction between XRCC4 and the catalytic domain of PNKP. Moreover, we show that phosphorylation of XRCC4 profoundly alters its binding to PNKP, and the two modes of binding lead to dramatically different responses to PNKP interaction with DNA and PNKP

* This work was supported by Canadian Institutes of Health Research Grants 15385 (to M. W.) and 13639 (to S. P. L.-M.) and Alberta Cancer Foundation Grant 23817 (to S. P. L.-M. and M. W.). This work was also supported, in whole or in part, by National Institutes of Health Grant CA 84442 (to D. A. R.).

[S] The on-line version of this article (available at http://www.jbc.org) contains supplemental text and Figs. S1–S10.

[1] Scientist of the Alberta Heritage Foundation for Medical Research. Engineered Air Chair in Cancer Research at the University of Calgary. To whom correspondence may be addressed: Southern Alberta Cancer Research Institute, University of Calgary, 3330 Hospital Dr. NW, Calgary, AB T2N 4N1, Canada. Fax: 403-283-8727; E-mail: leesmill@ucalgary.ca.

[2] To whom correspondence may be addressed: Cross Cancer Institute, 11560 University Ave., Edmonton, AB T6G 1Z2, Canada. Fax: 780-432-8428; E-mail: michaelw@cancerboard.ab.ca.

[3] The abbreviations used are: DSB, double-strand break; AC, acrylodan; FHA domain, forkhead-associated domain; NHEJ, nonhomologous end joining; PNKP, polynucleotide kinase/phosphatase; pXRCC4, XRCC4 phosphorylated at threonine 233; X4·LIV, XRCC4·DNA ligase IV complex.

kinase activity. Our data suggest that cellular XRCC4 exists in phosphorylated and nonphosphorylated forms and that not all of the cellular XRCC4 is in complex with DNA ligase IV. Intriguingly, both nonphosphorylated XRCC4 and the XRCC4·DNA ligase IV complex (X4·LIV) stimulate PNKP kinase activity, whereas CK2-phosphorylated XRCC4 (in the absence of DNA ligase IV) inhibited PNKP activity. Together, our data suggest that XRCC4 phosphorylation and complexation have subtle effects on PNKP activity and reveal new potential roles for XRCC4 and PNKP in NHEJ.

EXPERIMENTAL PROCEDURES

Expression and Purification of Proteins—Descriptions of the bacterial expression and purification of wild type and mutant human XRCC4 and PNKP are provided in the supplemental materials. XRCC4·DNA ligase IV complex (X4·LIV) and XRCC4-T233A·DNA ligase IV complex (X4T233A·LIV) were expressed in baculovirus-infected insect cells and purified as described previously (16).

In Vitro Phosphorylation of XRCC4—CK2α (17) with a GST tag was expressed in bacteria and purified over glutathione-Sepharose beads as described for GST-XRCC4 (see the supplemental materials), and the purified Sepharose bead-bound enzyme was used in phosphorylation reactions. For production of phosphorylated XRCC4 for biophysical characterization, phosphorylation reactions contained 5 mg of purified XRCC4 in 50 mM Tris-HCl, pH 7.5, 100 mM NaCl, 5 mM $MgCl_2$, and 1 mM ATP. The ratio of XRCC4 to CK2 used was 5:1, and the reactions were carried out at 30 °C for 2 h. At the end of the reaction, immobilized CK2 was removed by centrifugation at 1000 × *g*, and the resulting supernatant was concentrated ~5-fold using an ultrafiltration unit (30-kDa cutoff) and then dialyzed into 50 mM Tris-HCl, pH 8.0, containing 1 mM DTT and protease inhibitors as above. To determine the stoichiometry of phosphorylation, a small aliquot of the reaction was removed prior to the addition of ATP and incubated with radioactively labeled ATP (specific activity, ~200 cpm/pmol). For phosphorylation of WT and XRCC4-T233A for characterization of the phosphospecific antibody to Thr-233, the reactions contained 1.5 μg of purified XRCC4 protein, and reaction volumes and the amounts of CK2 were scaled down accordingly.

To examine the interference of DNA and/or PNKP on CK2 phosphorylation of XRCC4, 50 pmol of XRCC4, PNKP, and 45-bp phosphorylated duplex DNA were preincubated in a 20-μl reaction mixture containing 50 mM Tris-HCl, pH 7.5, 100 mM NaCl, 5 mM $MgCl_2$ for 10 min at 30 °C. The reactions were started by the addition of 0.2 μg of GST-CK2 and 1 mM ATP containing stabilized [γ-^{32}P]ATP (specific activity, ~500 cpm/pmol) and incubated for 5 or 10 min at 30 °C. The reactions were terminated by the addition of SDS (to 1%) and DTT (to 10 mM). The samples were heated to 100 °C for 3 min and then analyzed by autoradiography after SDS-PAGE on a 10% polyacrylamide gel.

Steady-state Fluorescence Studies—Steady-state fluorescence spectra were measured at 25 °C on a PerkinElmer Life Sciences LS-55 spectrofluorometer with 5-nm spectral resolution for excitation and emission as described in our earlier studies (18, 19). Unless otherwise stated, each protein was used at a concentration of 0.1 μM. The duplex DNA, supplied by Integrated DNA Technologies (Coralville, IA), had the sequences: 5′-GGC CAG CTA GTG GTG GTG GGC GCC GGC GGT GTG GGC ATT CGT AAT-3′ and 3′-CCG GTC GAT CAC CAC CAC CCG CGG CCG CCA CAC CCG TAA GCA TTA-5′. The lower strand was used as the single-stranded substrate. GraphPad Prism software was used for the analysis of binding data.

Sedimentation Equilibrium—The details of our protocol are described in the supplemental materials.

Circular Dichroism Spectroscopy—CD measurements were performed with an Olis DSM 17CD spectropolarimeter (Bogart, GA) as described previously (18). Protein concentrations used for each determination are presented in the corresponding figure legends.

PNKP Kinase Activity Assays—PNKP (1.5 μg) was premixed with 1.0 or 2.0 μg of XRCC4 or pXRCC4 and incubated at 37 °C for 5 min and then added to a reaction mixture (20 μl of total volume) containing kinase buffer (80 mM succinic acid, pH 5.5, 10 mM $MgCl_2$, and 1 mM DTT), 2 μM 45-bp duplex DNA substrate, and 3.3 pmol of [γ-^{32}P]ATP (PerkinElmer Life Sciences) and incubated for 20 min at 37 °C. Four μl of the sample was mixed with 2 μl of 3× sequencing gel loading dye (Fisher), boiled for 10 min, and run on a 12% polyacrylamide gel containing 7 M urea at 200 V. The gel was scanned on a Typhoon 9400 variable mode imager (GE Healthcare), and the resulting bands were quantified using ImageQuant 5.2 (GE Healthcare).

The influence of XRCC4 and pXRCC4 on the kinase activity of PNKP under limiting enzyme conditions was carried out as described in our previous publication with PNKP and XRCC1 (19). Briefly, two 50-μl reaction mixtures containing kinase buffer (80 mM succinic acid, pH 5.5, 10 mM $MgCl_2$, and 1 mM DTT), 0.4 nmol of DNA substrate, 0.4 nmol of unlabeled ATP, 3.3 pmol of [γ-^{32}P]ATP, and 0.5 μg of PNKP were incubated at 37 °C. Aliquots (3 μl) were taken from one of the reaction mixtures after incubation intervals of 0, 1, 2, 5, 10, 20, or 30 min. To the other reaction mixture, 4.0 μg of XRCC4 or pXRCC4 was added after a 20-min incubation, and then 3-μl aliquots were taken after additional time intervals. The samples were mixed with sequencing gel loading dye and analyzed as described above. The same procedure was followed to measure the influence of the X4·LIV complexes on PNKP kinase activity except that 5 μg of the complex was added 20 min after the start of the kinase reaction.

Measurement of Cellular Content of Proteins—To determine the relative amount of each protein, purified proteins were first quantitated by running on SDS-PAGE; then gels were stained with Coomassie Brilliant Blue, and the bands were compared with known amounts of BSA. HeLa cells were grown to ~80% confluence in DMEM with 10% fetal bovine serum in a humidified atmosphere of 5% CO_2 at 37 °C. To generate whole cell extracts, the cells were removed from plates by trypsinization, washed with ice-cold PBS, and then resuspended in ice-cold lysis NETN buffer (50 mM Tris-HCl, pH 7.5, 150 mM NaCl, 1 mM EDTA, 1% (v/v) Nonidet P-40, 1 μM microcystin-LR, plus protease inhibitors 0.2 μM phenylmethylsulfonyl fluoride, 0.2 μg/ml leupeptin, 0.2 μg/ml aprotinin, 0.2 μg/ml pepstatin). After incubation on ice for 30 min, the extracts were sonicated

and then clarified by centrifugation (10,000 rpm at 4 °C for 10 min). The pellet was extracted two more times with fresh lysis buffer as above, and the final supernatants were combined. Protein concentrations were determined using the detergent compatible protein assay (Bio-Rad) using BSA as standard. The amount of each protein in cell extracts was determined by Western blot using the purified proteins as standards. Immunoblots were quantified using ImageQuant software. At least three separate cell extracts were used for each experiment. Representative immunoblots are shown.

PNKP Expression in Mammalian Cells—Vectors for expression of N-terminal HA epitope-tagged PNKP and HA-tagged R35A-PNKP are described in the supplemental materials. HeLa cells were transfected with 3 μg of either vector control or vector encoding HA-tagged PNKP (pIRESpuro3-HA-PNKP) or HA-tagged R35A-PNKP (pIRESpuro3-HA-PNK-R35A). Transfections were carried out using Lipofectamine 2000 (Invitrogen), according to the manufacturer's recommended conditions, except that 10 μl of Lipofectamine reagent was used per 1.2×10^6 cells.

Immunoprecipitation Reactions—For immunoprecipitation of endogenous XRCC4 from HeLa cells, HeLa cells were grown and harvested, and NETN lysates were generated as described above. Two mg of extract was precleared using protein G-Sepharose beads (GE Healthcare), and XRCC4 was immunoprecipitated by incubation overnight at 4 °C with mouse polyclonal antisera to XRCC4 that had been covalently coupled to protein G-Sepharose beads (20). The beads were washed five times with 1 ml of lysis buffer, and immunoprecipitates were analyzed by SDS-PAGE and probed for XRCC4 or Thr-233-phosphorylated XRCC4 as indicated. For immunoprecipitation of transfected proteins, 72 h after transfection, the cells were lysed by incubation on ice for 30 min in HEPES/Nonidet P-40 lysis buffer (40 mM HEPES, pH7.5, 1 mM EDTA, 50 mM NaCl, 0.1% (v/v) Nonidet P-40) containing 0.2 μM phenylmethylsulfonyl fluoride, 0.2 μg/ml leupeptin, 0.2 μg/ml aprotinin, 0.2 μg/ml pepstatin, and 1 μM microcystin-LR, followed by sonication. Where indicated, the protein cross-linker dithiobis(succinimidyl propionate) (Thermo Scientific, Waltham, MA) was added to 1 mM final concentration, and extracts were incubated at room temperature for 30 min. The reactions were stopped by the addition of Tris-HCl, pH 7.5, to 50 mM followed by incubation for a further 15 min at room temperature. The extracts were then precleared with protein G-Sepharose, and XRCC4 or HA-PNKP was immunoprecipitated from 1.5 mg of extract as described above. The beads were washed five times with 1 ml of low salt/low detergent NETN buffer (50 mM Tris-HCl, pH 7.5, 5 mM EDTA, 50 mM NaCl, 0.1% (v/v) Nonidet P-40, 0.2 mM phenylmethylsulfonyl fluoride) and analyzed by SDS-PAGE and immunoblot as indicated.

RESULTS

Nonphosphorylated XRCC4 Co-immunoprecipitates with PNKP in Vitro—XRCC4 is regarded as a scaffold protein that plays a critical role in NHEJ. Previous studies have revealed that PNKP interacts with Thr-233-phosphorylated XRCC4 via its N-terminal FHA domain (7), suggesting that PNKP is recruited to DSBs with the XRCC4·DNA ligase IV complex. In preliminary studies, we observed that purified recombinant XRCC4 produced in *Escherichia coli* co-immunoprecipitated with PNKP, suggesting that these two proteins were also capable of interacting in a phosphorylation-independent manner (supplemental Fig. S1). This observation prompted us to examine the interaction of PNKP with both phospho- and non-phospho-XRCC4 in more detail. XRCC4 was expressed and purified from *E. coli*. To ensure that the purified protein did not contain residual phosphorylation sites and that it was not contaminated with DNA, where indicated, XRCC4 was treated with phosphatase and ethidium bromide before use (see supplemental materials for details). Unphosphorylated XRCC4 is referred to as XRCC4. Despite having a molecular mass of ~38,000 Da, based on its amino acid sequence, XRCC4 migrated on SDS-PAGE with an apparent molecular mass of ~55,000 Da (supplemental Fig. S2*A*), consistent with published values (3, 12). The observed anomalous mobility of recombinant XRCC4 in SDS-PAGE is likely due to its low isoelectric point (21, 22). Where indicated, XRCC4 was phosphorylated *in vitro* by CK2 and is referred to as pXRCC4. The stoichiometry of phosphorylation was ~1 mol of phosphate/mol of XRCC4 (supplemental Fig. S2, *B* and *C*). As expected, pXRCC4 migrated slightly more slowly on SDS-PAGE than unphosphorylated XRCC4 (supplemental Fig. S2*B*).

PNKP Interacts with Non-phospho-XRCC4 in Solution—To further study the interaction between PNKP and pXRCC4 and XRCC4, we used the covalent sulfhydryl-specific environment-sensitive fluorescent probe acrylodan (AC) (23) to label PNKP. PNKP-AC retained ~90% of its kinase activity compared with unlabeled PNKP (18). The PNKP-AC·pXRCC4 interaction was accompanied by partial quenching of AC fluorescence (excitation at 380 nm) with no change in the emission maximum (~485 nm). The binding affinity, K_d, was determined by following fluorescence quenching as a function of pXRCC4 concentration. A plot of relative fluorescence intensities *versus* concentration of pXRCC4 is shown in Fig. 1*A* (*inset*). Nonlinear regression analysis of the binding data yielded a K_d value of 5 ± 1 nM. A similar analysis of interaction between PNKP-AC with XRCC4 indicated that XRCC4 bound PNKP-AC, but with a lower affinity (K_d 90 ± 5 nM) (Fig. 1*B*). These data confirm that PNKP interacts with XRCC4 in a non-phosphorylation-dependent manner *in vitro*.

XRCC4 Interacts with the Catalytic Domain of PNKP—Previous studies have shown that pXRCC4 binds to the FHA domain of PNKP (7). To obtain quantitative data for this interaction, we purified the $PNKP^{FHA}$ domain (residues 1–130) and labeled the single Cys residue (Cys-46) with AC. When the labeled protein $PNKP^{FHA\text{-}AC}$ was excited at 380 nm, the emission maximum occurred at 495 nm, and the addition of pXRCC4 resulted in AC fluorescence quenching (Fig. 1*C*). Titration of $PNKP^{FHA\text{-}AC}$ with pXRCC4 provided a K_d value of 4 ± 1 nM, in close agreement with the value obtained with the full-length PNKP protein. In contrast, the addition of XRCC4 had no significant effect on AC fluorescence (Fig. 1*D*), indicating that unphosphorylated XRCC4 does not interact with the FHA domain of PNKP.

We next asked whether the interaction of PNKP and unphosphorylated XRCC4 is mediated by the C-terminal catalytic

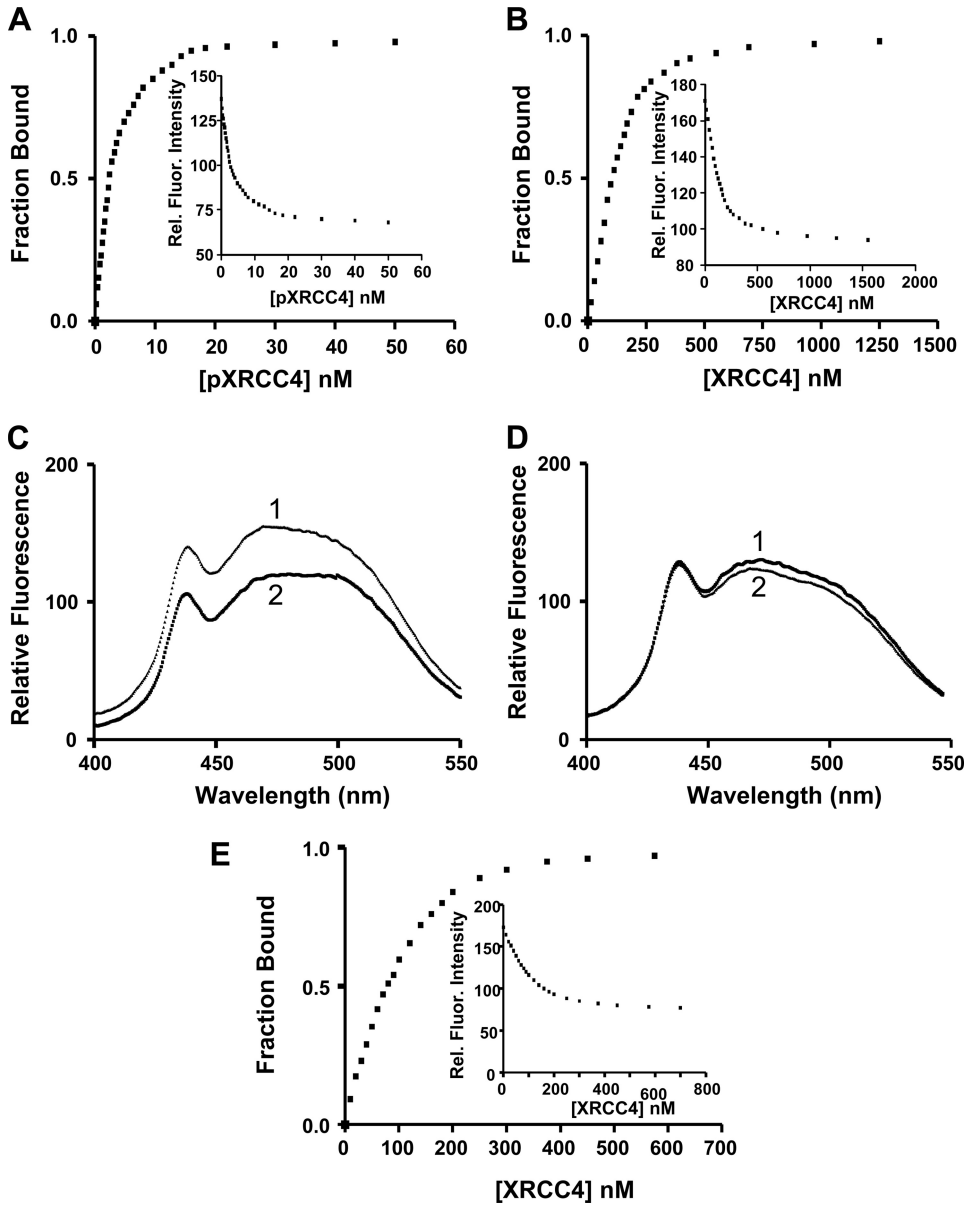

FIGURE 1. **Phosphorylation of XRCC4 alters its mode of binding to PNKP.** *A* and *B*, fluorescence titration of PNKP-AC *versus* pXRCC4 and XRCC4. Labeled PNKP (0.3 μM) was excited at 380 nm, and the relative fluorescence (*Rel. Fluor.*) intensities were monitored at 480 nm (see *insets*). The fraction of PNKP-AC bound *versus* pXRCC4 (*A*) and XRCC4 (*B*) concentration is plotted, revealing considerably tighter binding of PNKP to pXRCC4. *C* and *D*, effect of pXRCC4 and XRCC4 on $PNKP^{FHA\text{-}AC}$ fluorescence. $PNKP^{FHA\text{-}AC}$ was excited at 380 nm, and the effect of pXRCC4 (*C*) and XRCC4 (*D*) on the emission fluorescence was determined. In each figure the upper (*line 1*) and lower (*line 2*) signals show the fluorescence spectrum for $PNKP^{FHA\text{-}AC}$ in the absence or presence of XRCC4, respectively. *E*, fluorescence titration of $PNKP^{CT\text{-}AC}$ *versus* XRCC4. Labeled $PNKP^{CT\text{-}AC}$ was excited at 380 nm, and the relative fluorescence intensity was monitored at 480 nm (see *inset*). The fraction of $PNKP^{CT\text{-}AC}$ bound *versus* XRCC4 concentration is plotted.

kinase/phosphatase domain of PNKP. A C-terminal fragment of PNKP corresponding to amino acids Lys-141 to Gly-521 was expressed in *E. coli*, purified, and similarly labeled with AC ($PNKP^{CT\text{-}AC}$). When the labeled protein was excited at 380 nm, the emission maximum centered ~485 nm. The addition of XRCC4 resulted in partial quenching of AC fluorescence and amounted to ~13% when the two proteins were mixed in a 1:1 molar ratio. Fluorescence titration (Fig. 1*E*) yielded a K_d value of 100 ± 10 nM, in close agreement with the K_d value obtained with full-length PNKP. The addition of pXRCC4 induced ~8% quenching of AC fluorescence, signifying interaction between the two proteins, but this level of quenching was not sufficient to allow us to determine a K_d value. Thus, non-phospho-XRCC4 interacts with the C-terminal catalytic domain of PNKP, whereas Thr-233-phosphorylated XRCC4 interacts primarily with the FHA domain of PNKP.

Interaction of PNKP with Both Phospho- and Non-phospho-XRCC4 Produces a Conformational Change in Both Proteins—The influence of CK2 phosphorylation on the biophysical properties of XRCC4 was examined by sedimentation equilibrium analysis and CD. The data presented in supplemental Figs. S3 and S4 and Table S1 indicate that phosphorylation of XRCC4 shifts its dimer-tetramer equilibrium more toward the dimeric state and increases the proportion of random structure found in the protein (Table 1).

We next used CD to determine whether the interaction of PNKP with either pXRCC4 or XRCC4 affected the secondary structure of either protein. Because the observed ellipticity is an additive parameter, one can generate the theoretical CD spectrum for a mixture of proteins by adding together the spectra of individual proteins, and this spectrum can be compared with that observed experimentally to see whether the interaction has induced any conformational change. The far-UV CD spectra obtained for the [PNKP·XRCC4] and [PNKP·pXRCC4] complexes (1:1 molar ratios) are shown in Fig. 2 (*A* and *B*). The experimentally observed ellipticity values deviate from the theoretical values particularly in the 209- and 218-nm wavelength regions, demonstrating that the interaction has produced a conformational change in both complexes. For instance, for the [PNKP·XRCC4] complex, the difference between the observed and the theoretical ellipticity values at 209 nm was ~2000 deg cm^2 $dmol^{-1}$, whereas the experimental error in these measurements is only ±300 deg cm^2 $dmol^{-1}$. Comparison of the secondary structure of the complexes with the secondary structures of the individual proteins (Table 1) suggests that the interaction between PNKP and XRCC4 resulted in an increase in the random structure, whereas the [PNKP·pXRCC4] complex assumes a slightly higher α-helical content at the expense

of the random structure. These two protein complexes exist in different conformational states, and this could arise from the nature of their interactions. For instance, if XRCC4 binds to the catalytic domain of PNKP while pXRCC4 associates with the FHA domain, the two complexes would assume different secondary structures.

Far-UV CD experiments also provided additional evidence for interaction between the $PNKP^{CT}$ domain and XRCC4 and pXRCC4. When the two proteins $PNKP^{CT}$ and XRCC4 or $PNKP^{CT}$ and pXRCC4 were mixed in 1:1 molar ratio, the experimentally observed CD spectra deviated from the calculated theoretical CD spectra for the complexes (Fig. 2, *C* and *D*, and Table 1). Together these data suggest that interaction of PNKP with XRCC4 produces a conformational change.

TABLE 1
Secondary structural analysis of XRCC4, PNKP, pXRCC4, XRCC4·PNKP, and pXRCC4·PNKP complexes

Protein	Molar ellipticity		α-Helix[a]	β-Structure[a]	Random[a]
	$[\theta]_{209\ nm}$	$[\theta]_{218\ nm}$			
			%	%	%
XRCC4	−12,400	−10,600	32	30	38
pXRCC4	−11,400	−9,800	32	23	45
PNKP	−10,100	−9,250	25	55	20
XRCC4·PNKP[b]	−9,500	−9,000(E)[c]			
	−11,300	−10,000(T)	26	35	39
pXRCC4·PNKP[b]	−9,100	−82,00(E)			
	−10,800	−9,600(T)	32	34	34

[a] Analysis of the CD spectra according to the method of Chen *et al.* (38).
[b] The two proteins in the XRCC4·PNKP and pXRCC4·PNKP mixtures were mixed in a 1:1 molar ratio.
[c] E represents experimental values, and T represents theoretical values assuming no protein-protein interaction.

Interaction of PNKP, XRCC4, and pXRCC4 with DNA—Given that the natural substrate for PNKP is DNA, we asked whether interaction of PNKP with XRCC4 affected its affinity for DNA. Because XRCC4 has also been reported to interact with DNA (3), we first examined the binding of each protein individually to DNA. Quantitative data for the binding of a blunt-ended 45-mer DNA duplex to XRCC4 and pXRCC4 was obtained by measuring the quenching of the intrinsic Trp fluorescence of the proteins at 342 nm following excitation at 295 nm as a function of DNA concentration. Binding of the 45-mer DNA duplex to XRCC4 and pXRCC4 resulted in partial quenching of Trp fluorescence with no change in emission maximum, which enabled determination of binding affinities by following fluorescence quenching as a function of 45-mer DNA duplex concentration. A representative plot of relative fluorescence intensity *versus* the concentration of duplex DNA for XRCC4 and pXRCC4 is shown in Fig. 3 (*inset*). Nonlinear regression analysis of the binding data revealed unimodal binding with K_d values of 0.28 ± 0.03 μM for XRCC4 and 0.50 ± 0.05 μM for pXRCC4, respectively, indicating that phosphorylation by CK2 did not have a major effect on the interaction of XRCC4 with double-stranded DNA.

Because radiation-induced DSBs often contain single-stranded termini, we also studied the binding of the unphosphorylated and 5′-phosphorylated single-stranded 45-mer oligonucleotide to XRCC4 and found that the protein bound both oligonucleotides with similar affinities (0.70 ± 0.05 and 0.80 ± 0.05 μM, respectively). Hence, XRCC4 exhibits higher affinity (~2.5-fold) for double-stranded oligonucleotides compared with single-stranded oligonucleotides and is not influenced by the phosphorylation status of the DNA. Similar analysis afforded K_d values of 0.5 and 2.6 μM for PNKP binding to 45-mer duplex with 5′-OH and 5′-phosphate termini, respectively (data not shown).

We next determined the interaction of pXRCC4 with DNA in the presence of PNKP. For these studies, PNKP was labeled with AC as described above, and the extent of AC fluorescence quenching induced by various combinations of pXRCC4, PNKP, and duplex DNA (1:1 molar ratio with protein) was determined (Table 2). (To produce the complexes in a nearly quantitative fashion, a 2-fold excess of duplex DNA (1 μM) was added to study the effect of DNA binding on PNKP-AC (0.5 μM) in the absence and presence of pXRCC4. The concentration of duplex DNA added was higher than its K_d value for PNKP (0.28 μM).) The addition of DNA to PNKP-AC produced ~11%

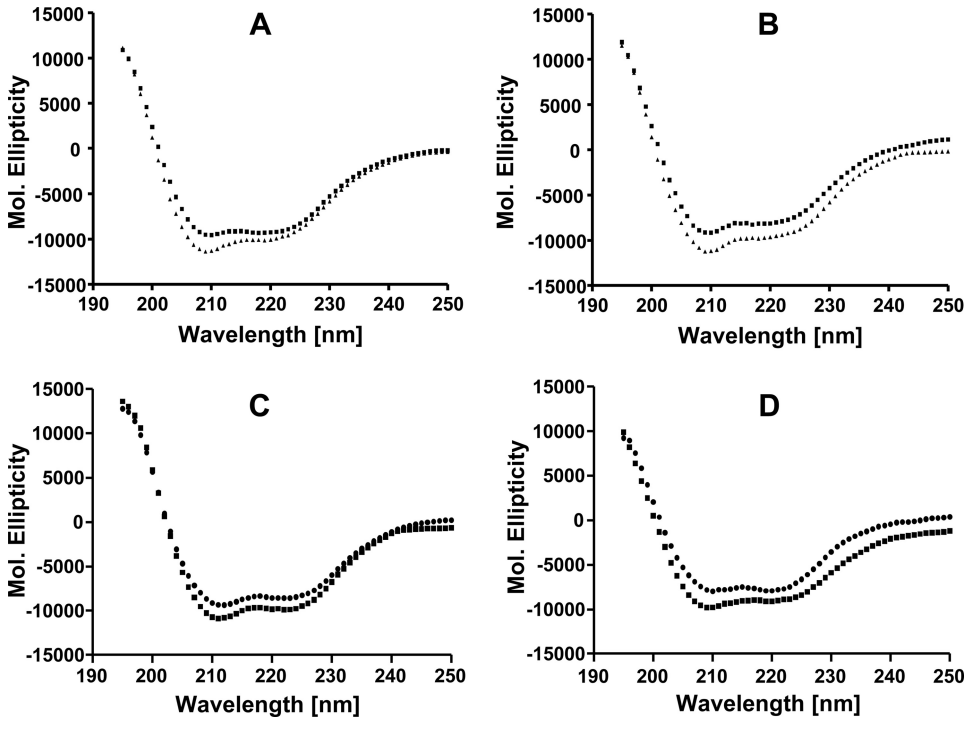

FIGURE 2. **Interaction of PNKP with both phospho- and non-phospho-XRCC4 produces a conformational change in both proteins.** *A*, far-UV CD spectrum of pXRCC4·PNKP complex (0.55 mg/ml total protein) in sample buffer (■) and the theoretical CD spectrum for an equimolar mixture of these two proteins (▲). *B*, XRCC4·PNKP complex (0.5 mg/ml) (■) and the corresponding theoretical CD spectrum for an equimolar mixture of these two proteins (▲). *C*, far-UV CD spectrum of $PNKP^{CT}$·XRCC4 complex (0.55 mg/ml) (■) and the theoretical CD spectrum for an equimolar mixture of these two proteins (●). *D*, $PNKP^{CT}$·pXRCC4 complex (0.6 mg/ml) (■) and the corresponding theoretical CD spectrum (●).

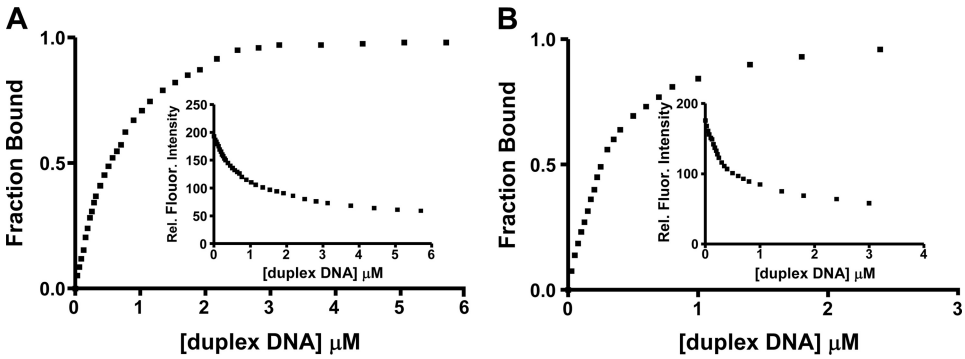

FIGURE 3. **Fluorescence titration of pXRCC4 and XRCC4 with duplex (45-mer) DNA.** *A* and *B*, pXRCC4 (*A*, 0.5 μM) and XRCC4 (*B*, 0.5 μM) in 50 mM Tris-HCl, pH 7.5, 100 mM NaCl, and 5 mM $MgCl_2$ were excited at 295 nm, and the fluorescence intensity was monitored at 332 nm (see *inset*). The fraction bound, *i.e.* relative fluorescence (*Rel. Fluor.*) intensity *versus* ligand concentration, is plotted.

TABLE 2
Effect of pXRCC4 and duplex DNA binding on AC fluorescence of labeled PNKP and $PNKP^{FHA}$ in the absence and presence of each other

Complex	Quenching[a]
PNKP + duplex DNA	11 ± 1
[PNKP·duplex DNA] + pXRCC4	13 ± 2
PNKP + pXRCC4	15 ± 2
PNKP + [duplex DNA·pXRCC4]	14 ± 2
[PNKP·pXRCC4] + duplex DNA	2 ± 1
$PNKP^{FHA}$ + duplex DNA	2 ± 1
$PNKP^{FHA}$ + pXRCC4	18 ± 2
$PNKP^{FHA}$ + [pXRCC4·duplex DNA]	16 ± 2
[$PNKP^{FHA}$·pXRCC4] + duplex DNA	2 ± 1
[$PNKP^{FHA}$·duplex DNA] + pXRCC4	16 ± 2
[PNKP·pXRCC4]^{unlabeled} + duplex DNA	18 ± 2

[a] A 2-fold excess of duplex DNA (1 μM) was added to PNKP-AC (0.5 μM). Labeled PNKP and pXRCC4 were in equimolar concentration. The labeled protein, PNKP-AC or $PNKP^{FHA-AC}$, was excited at 380 nm, and the effect of pXRCC4 and duplex DNA binding on AC fluorescence was monitored at 485 nm. The decrease in total fluorescence intensity at 485 nm is reported as percent quenching. The values represent the means ± S.E. (n = 3). The brackets indicate complexes.

quenching of AC fluorescence intensity, whereas the addition of pXRCC4 to PNKP-AC resulted in ~15% quenching. Because pXRCC4 can bind duplex DNA (K_d = 0.50 μM), we wanted to see whether preincubation of pXRCC4 with DNA, to allow formation of a binary complex [pXRCC4·DNA], would affect binding to PNKP-AC. The addition of the [pXRCC4·DNA] complex produced ~14% quenching in AC fluorescence intensity, thus demonstrating that PNKP-AC can bind to this binary complex to form a ternary complex. Likewise, the addition of pXRCC4 to the complex of PNKP-AC bound to DNA, [PNKP-AC·DNA], induced ~13% further quenching in AC fluorescence, thus similarly providing evidence for the formation of a ternary complex. However, no significant additional quenching of AC fluorescence was observed when the DNA was added to the [PNKP-AC·pXRCC4] binary complex. Hence, when pXRCC4 was bound to PNKP, the DNA was unable to bind to PNKP and remained free or was bound to pXRCC4 in such a way that it did not perturb the AC fluorescence of PNKP. In contrast, duplex DNA was capable of binding to the complex of PNKP with nonphosphorylated XRCC4 [PNKP-AC·XRCC4] (~20% quenching), suggesting that XRCC4 and pXRCC4 affect PNKP DNA binding in opposite ways. To determine whether the duplex DNA bound to [PNKP·pXRCC4], we mixed the unlabeled proteins PNKP and pXRCC4 in 1:1 molar ratio and studied the effect of adding the DNA on the intrinsic Trp fluorescence of the protein complex. The addition of DNA to this complex produced ~18% quenching in Trp fluorescence, thus clearly demonstrating that DNA binds to the [PNKP·pXRCC4] complex through interaction with pXRCC4.

Confirmation that pXRCC4 maintains binding to DNA while bound to PNKP was shown by analysis of complex formation involving $PNKP^{FHA-AC}$, pXRCC4, and DNA. The addition of DNA had no significant effect on AC fluorescence of $PNKP^{FHA-AC}$, which is not surprising because the DNA-binding sites of PNKP are located in the C-terminal catalytic domain. Binding of pXRCC4 to $PNKP^{FHA-AC}$ induced ~18% quenching in AC fluorescence, and the addition of the binary complex [pXRCC4·DNA] produced ~16% quenching in fluorescence intensity, providing evidence for the formation of a ternary complex involving $PNKP^{FHA}$, pXRCC4, and the duplex DNA (Table 2). In contrast, the addition of DNA to the binary complex [$PNKP^{FHA-AC}$·pXRCC4] caused no change in AC fluorescence, probably because the DNA binding site on pXRCC4 is situated far from the Thr(P)-233 residue associated with PNKP binding.

Interaction of PNKP with Phosphorylated XRCC4 Inhibits the Kinase Activity of PNKP—The results of our fluorescence studies suggested that DNA was unable to bind to PNKP when PNKP was complexed with pXRCC4. We therefore carried out kinase activity measurements of PNKP in the absence and presence of pXRCC4 with the implication that the failure of PNKP to bind to DNA would abrogate PNKP kinase activity. When PNKP was mixed with pXRCC4 in a 1:1 molar ratio prior to adding the 45-mer duplex DNA, the observed kinase activity of this binary complex was ~20% compared with the activity of PNKP alone (Fig. 4*A*), and when the two proteins were mixed in a 1:2 molar ratio, the observed activity of this complex was further reduced to ~10% of PNKP activity. In this assay, the DNA concentration was ~20-fold in excess of the PNKP, suggesting that the PNKP remained tightly bound to the pXRCC4, because it would otherwise have been able to phosphorylate the DNA. However, when PNKP was mixed with XRCC4 in 1:1 and 1:2 molar ratios prior to adding the DNA, the observed kinase activities were similar to the control levels (~ 90 and ~85%, respectively). In a follow-up experiment, we preincubated XRCC4 or pXRCC4 with DNA for 5 min at 37 °C prior to the addition of PNKP for the kinase assay. Under these conditions, XRCC4 had no significant effect on PNKP activity, suggesting that the DNA had access to PNKP, whereas when the DNA was complexed with pXRCC4, it had very limited access to PNKP because pXRCC4 again inhibited ~90% of PNKP kinase activity (Fig. 4*B*). As a further control for nonspecific inhibition of DNA kinase activity, including the possible presence of residual unlabeled ATP, the pXRCC4 was mixed with phage T4 polynucleotide kinase, but no inhibition of the T4 kinase activity was observed (supplemental Fig. S5).

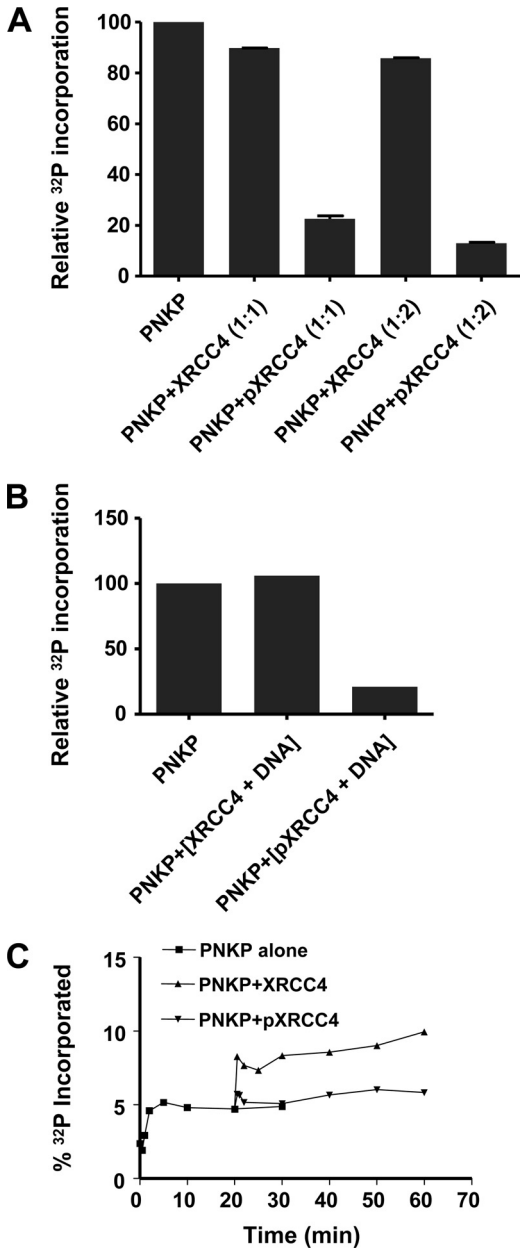

FIGURE 4. **pXRCC4 inhibits the DNA kinase activity of PNKP.** *A*, XRCC4 and pXRCC4 were added to PNKP and incubated for 5 min at 37 °C prior to starting the assays. The molar ratios of PNKP to XRCC4 or pXRCC4 used were 1:1 and 1:2, respectively. The kinase activity is expressed as relative ^{32}P incorporated, taking the value for reaction with PNKP alone as 100%. *B*, XRCC4 and pXRCC4 were added to 45-mer duplex DNA and incubated for 5 min at 37 °C prior to the measurement of kinase activity. *C*, XRCC4 but not pXRCC4 influences the kinetics of phosphorylated product accumulation. The concentration of 45-mer duplex DNA was 4 μM, and the PNKP concentration was 0.35 μM. At 20 min of incubation, 0.70 μM of XRCC4 or pXRCC4 were added. The assays were carried out four times as described under "Experimental Procedures," and a representative plot is shown.

XRCC4 but Not pXRCC4 Stimulates Enzymatic Turnover of PNKP—To further define a role for the XRCC4·PNKP interaction, we examined the effect of XRCC4 and pXRCC4 on the turnover of PNKP. The kinase activity of PNKP was assayed using a limited concentration of the enzyme with 45-mer duplex and [γ-^{32}P]ATP (Fig. 4*C*). The rate of product accumulation decreased over the course of the assay and reached a plateau after ~10 min. The addition of XRCC4 at 20 min (*i.e.* in the plateau region) resulted in reactivation of kinase activity, and the percentage of ^{32}P incorporated nearly doubled. The observed increase in kinase activity was due to PNKP because XRCC4 itself has no kinase activity. Thus, the addition of XRCC4 stimulated the turnover of the enzyme-product adduct. PNKP and XRCC4 exhibit similar binding affinities for duplex 45-mer (5′-OH) (K_d values of 0.5 and 0.25 μM for PNKP and XRCC4, respectively), but they had different binding affinities for duplex 45-mer (5′-phosphate), which can be considered a product of the enzymatic reaction of PNKP. XRCC4 exhibited higher affinity than PNKP for 5′-phosphorylated DNA, with K_d values of 0.5 and 2.8 μM, respectively, a difference of ~5-fold. Hence, it is conceivable that XRCC4 binds to [PNKP·DNA] binary complex and releases the product (bound phosphorylated DNA) from PNKP by virtue of its higher affinity than PNKP, thus freeing the enzyme to continue its enzymatic activity. In marked contrast, when pXRCC4 was added to the enzymatic reaction mixture at 20 min in the plateau region, there was no significant reactivation of the kinase activity of PNKP. Thus, XRCC4 but not pXRCC4 stimulates PNKP enzymatic turnover.

The XRCC4·DNA Ligase IV Complex (X4·LIV) Stimulates PNKP Enzyme Turnover—XRCC4 interacts with the tandem BRCT domains of DNA ligase IV in a stable, phosphorylation-independent manner (13, 24, 25). Indeed, because XRCC4 stabilizes DNA ligase IV, it has been suggested that the cellular pool of DNA ligase IV is complexed with XRCC4. We therefore asked whether the X4·LIV complex affected PNKP activity in a similar manner to free XRCC4. For these experiments, the X4·LIV was expressed in baculovirus-infected insect cells. The protein content of the X4·LIV preparations is shown in supplemental Fig. S6. Significantly, X4·LIV complex purified from baculovirus infected insect cells did not inhibit PNKP kinase activity (Fig. 5*A*); indeed, it had a slightly stimulatory effect. It was therefore important to determine whether the X4·LIV complex was indeed phosphorylated on Thr-233. To do this, a phosphospecific antibody was generated and shown to be specific for Thr-233 *in vitro* (supplemental Fig. S7). Comparison with *in vitro* phosphorylated XRCC4 showed that baculovirus prepared X4·LIV was indeed phosphorylated at Thr-233 (supplemental Fig. S8). We therefore generated a X4·LIV complex in which Thr-233 had been mutated to alanine (X4T233A·LIV). Surprisingly, X4T233A·LIV stimulated PNKP to a similar extent as phospho-X4·LIV (Fig. 5*A*). Thus, in contrast to bacterially expressed, CK2-phosphorylated pXRCC4, Thr-233-phosphorylated XRCC4 in the context of the X4·LIV complex does not inhibit PNKP activity. We also examined the effect of baculovirus expressed X4·LIV complex on PNKP turnover. Significantly, both endogenously phosphorylated X4·LIV complex and X4T233A·LIV complex stimulated PNKP turnover to a similar extent (Fig. 5*B*).

XRCC4 Phosphorylation and Complexes in Human Cells—In summary, our data so far using bacterially expressed XRCC4 alone show that non-phospho-XRCC4 interacts with the catalytic domain of PNKP, and this interaction stimulates PNKP kinase activity, whereas interaction with pXRCC4 impedes PNKP phosphorylation of DNA. In contrast, baculovirus expressed X4·LIV complex stimulates PNKP enzymatic turn-

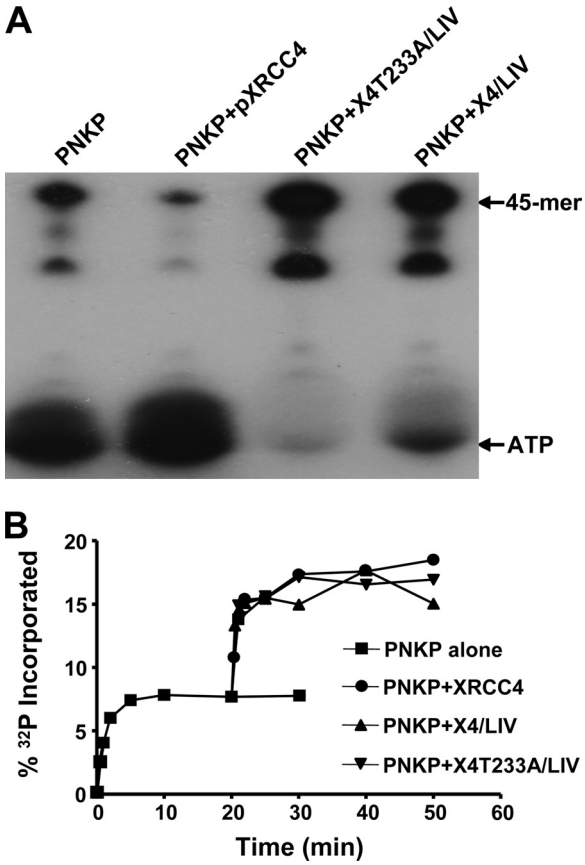

FIGURE 5. **Influence of XRCC4·DNA ligase IV complex on PNKP kinase activity.** *A*, pXRCC4, X4·LIV, and X4T233A·LIV were added to PNKP and incubated for 5 min at 37 °C prior to the measurement of kinase activity. The molar ratios of PNKP and pXRCC4 or complex used were 1:2. *B*, stimulation of PNKP kinase activity by XRCC4·DNA ligase IV complexes. We followed the conditions described under "Experimental Procedures."

TABLE 3
Estimation of relative amounts of XRCC4, DNA ligase IV, and PNKP in 50 μg of human (HeLa) cell extract

Protein	Amount	Molar quantity[a]
	ng	*pmol*
XRCC4	4.4 ± 1.4	0.117
DNA ligase IV	1.7 ± 0.5	0.017
PNKP	2.9 ± 0.1	0.052

[a] Molar quantities of XRCC4, DNA ligase IV, and PNKP were determined using molecular masses of 38,000, 104,000, and 57,100, respectively.

over activity regardless of Thr-233 phosphorylation status, and X4·LIV containing nonphosphorylated XRCC4 does not inhibit PNKP kinase activity. These new findings prompted us to investigate XRCC4 complex formation and phosphorylation in mammalian cells. We first estimated the relative levels of XRCC4, DNA ligase IV, and PNKP in HeLa cells. Whole cell extracts were generated, and the signals in immunoblots were compared with those of calibrated amounts of the purified proteins (supplemental Figs. S9 and S10 and Table 3). Our measurement of the cellular levels of XRCC4 indicated the presence of ~2 XRCC4 molecules to every PNKP molecule, as well as ~6-fold excess of XRCC4 relative to DNA ligase IV, suggesting that at the cellular level, a population of XRCC4 exists that is not complexed with DNA ligase IV and would therefore be available to interact with other NHEJ proteins, including PNKP.

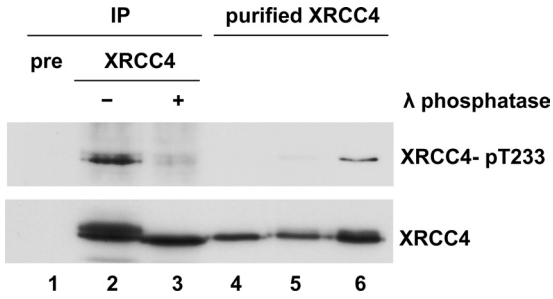

FIGURE 6. **Approximately 50% of endogenous XRCC4 is phosphorylated on Thr-233 *in vivo*.** XRCC4 was immunoprecipitated (*IP*) from HeLa cells, and immunoblots were probed with a phosphospecific antibody to Thr-233 or a polyclonal antibody to XRCC4 as indicated. *Lane 1*, contained a mock immunoprecipitation with preimmune serum (pre). *Lanes 2* and *3*, immunoprecipitated XRCC4. After immunoprecipitation, the sample in *lane 3* was incubated with λ phosphatase prior to SDS-PAGE. *Lane 4*, 40 ng of mock-phosphorylated XRCC4. *Lane 5*, 20 ng of CK2-phosphorylated XRCC4. *Lane 6*, 40 ng of CK2-phosphorylated XRCC4. The major Thr(P)-233 cross-reacting band (*upper panel*, *lane 2*) lined up with the lower band of the XRCC4 doublet (*lower panel*, *lane 2*).

We also examined the phosphorylation status of XRCC4 in cells. XRCC4 migrated as a doublet on SDS-PAGE that collapsed to a single band upon incubation with λ phosphatase, clearly indicating that the upper band of the XRCC4 doublet is due to phosphorylation (supplemental Fig. S10*B*). The ratio of the upper phosphorylated band to the lower band was ~50:50, suggesting that at least 50% of the cellular XRCC4 is phosphorylated. To determine the extent of Thr-233 phosphorylation of cellular XRCC4, XRCC4 was immunoprecipitated from HeLa cells, and immunoblots were probed for Thr-233 phosphorylation. Thr-233-phosphorylated XRCC4 was found predominantly in the lower band of the XRCC4 doublet (Fig. 6). Thus, at most approximately half of the cellular XRCC4 is phosphorylated on Thr-233. Neither the kinases responsible for phosphorylation of the upper band of the XRCC4 doublet nor the effects of these phosphorylation events are known; however, these results do suggest that a significant fraction of endogenous XRCC4 is not phosphorylated on Thr-233 and therefore could be available for interaction with PNKP in a non-FHA-mediated manner.

To determine whether PNKP interacted with XRCC4 in a non-FHA-dependent manner in cells, HeLa cells were transfected with either HA-tagged wild type PNKP or HA-tagged PNKP containing an alanine mutation at Arg-35 (HA-PNKP-R35A), a mutation that has been shown to ablate FHA domain function (7). The tagged WT and mutant PNKP were immunoprecipitated, and precipitates were probed for XRCC4. Because the interaction between PNKP and non-phospho-XRCC4 is relatively weak with a binding constant K_d of 90 nM (this study), extracts were treated with the thiol-cleavable cross-linker, dithiobis(succinimidyl propionate), prior to immunoprecipitation to stabilize protein-protein interactions (26). As shown in Fig. 7*A*, HA-PNKP-R35A immunoprecipitated endogenous XRCC4 in dithiobis(succinimidyl propionate)-treated extracts, consistent with an FHA-independent interaction between XRCC4 and PNKP. This interaction was specific for XRCC4 and FHA-mutated PNKP because no interaction was observed with the unrelated protein Mre11 (Fig. 7). In reciprocal reactions, we show that antibodies to XRCC4 immunoprecipitated

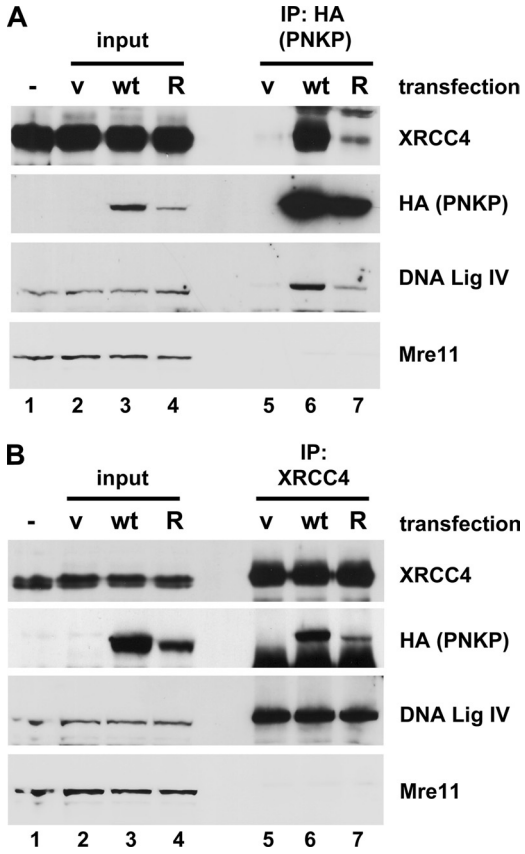

FIGURE 7. **PNKP interacts with XRCC4 in an FHA-independent manner.** HeLa cells were either untransfected (–, *lane 1*), transfected with vector alone (*v*, *lanes 2* and *5*), HA-tagged WT PNK (*wt*, *lanes 3* and *6*), or HA-tagged R35A-PNK (*R*, *lanes 4* and *7*). Seventy-two hours later, the cells were lysed, and extracts were incubated in the presence of dithiobis(succinimidyl propionate), a thiol cleavable protein cross-linker as described under "Experimental Procedures." *A*, HA-tagged PNKP was immunoprecipitated (*IP*), and immunoprecipitates were analyzed by SDS-PAGE and Western blot using antibodies to HA (PNKP), XRCC4, DNA ligase IV, or Mre11 (negative control) as indicated. *Lanes 2–4* contained 50 μg of extract preimmunoprecipitation (input). *Lane 1* contained 50 μg of whole cell extracts from untransfected HeLa cells. *B*, as in *A*, except endogenous XRCC4 was immunoprecipitated. The immunoblots were probed as indicated.

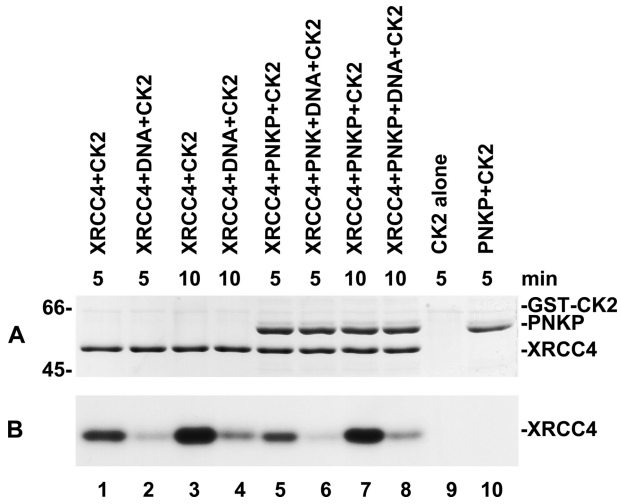

FIGURE 8. **Preincubation of XRCC4 with DNA inhibits phosphorylation of XRCC4 by CK2.** Purified XRCC4 (50 pmol) was incubated with 0. 2 μg of CK2 and [γ-^{32}P]ATP alone (*lanes 1* and *3*) or in the presence of 50 pmol 5′-phosphorylated duplex DNA (*lanes 2* and *4*), in the presence of 50 pmol PNKP (*lanes 5* and *7*), or in the presence of both DNA and PNKP (*lanes 6* and *8*) as described under "Experimental Procedures." The control lanes (*lanes 9* and *10*) show CK2 incubated alone with [γ-^{32}P]ATP or with additional PNKP. The reactions were analyzed on SDS-PAGE, and the gel was stained with Coomassie Blue (*A*) followed by autoradiography (*B*).

both WT PNKP and R35A-PNKP (Fig. 7*B*), again consistent with an FHA-independent interaction between XRCC4 and PNKP. Together, our cellular data show that (i) not all of the endogenous XRCC4 in human cells is phosphorylated on Thr-233; (ii) XRCC4 is present in excess of DNA ligase IV, suggesting that not all of the cellular XRCC4 is in complex with DNA ligase IV; and (iii) XRCC4 can interact with PNKP in an FHA-independent manner *in vivo*.

Phosphorylation of XRCC4 by CK2 in the Presence of DNA and PNKP—Like Koch *et al.* (7), we observed constitutive phosphorylation of XRCC4 at Thr-233 in unirradiated cells (Fig. 6 and supplemental Fig. S10), implying that Thr-233 phosphorylation does not require the presence of DNA DSBs. Moreover, phosphorylation of XRCC4 on Thr-233 did not increase after IR (data not shown), indicating that it is not DNA damage-inducible. However, these observations do not rule out the possibility that such phosphorylation may occur when XRCC4 is bound at DSBs. We therefore investigated whether human CK2 was capable of phosphorylating XRCC4 while bound to DNA and/or PNKP (Fig. 8). Preincubation of XRCC4 with PNKP had no significant effect on the extent of phosphorylation of XRCC4 compared with the phosphorylation of XRCC4 alone, but the presence of DNA dramatically inhibited CK2 activity, as has previously been shown for *Xenopus laevis* CK2 (27), and this was not ameliorated by the additional presence of PNKP.

DISCUSSION

PNKP is required to process unligatable strand break termini generated directly by many genotoxic agents (28) or as intermediates in repair pathways (29) and thus often plays a major role in DNA single- and double-strand break repair. The clinical importance of its activity has recently been emphasized by the discovery of an autosomal recessive disorder resulting from mutations in PNKP, which gives rise to microcephaly and seizures (30). Key partners of PNKP in single- and double-strand break repair are the scaffold proteins, XRCC1 and XRCC4, respectively. Although it is generally considered that interaction between PNKP and these proteins is mediated by the binding of CK2-phosphorylated scaffold protein to the FHA domain of PNKP (7, 31), we have recently shown that XRCC1 can interact with the catalytic domain of PNKP and stimulate PNKP activity (19, 32). These observations prompted us to examine the interactions between unphosphorylated XRCC4, CK2-phosphorylated XRCC4, and PNKP to improve our understanding of the mechanism by which these proteins function during NHEJ.

Biophysical Interactions of XRCC4 and pXRCC4 with PNKP—Our *in vitro* data clearly established a phosphorylation-independent interaction of bacterially expressed XRCC4 with PNKP and further indicated that XRCC4 and CK2-phosphorylated XRCC4 (pXRCC4) bind to PNKP at different sites. PNKP-AC exhibited strong affinity for pXRCC4 with a K_d value of 5.0 ± 1.0 nM, which was almost identical to the K_d value of 4.0 ± 1.0 nM obtained for the interaction of PNKP$^{FHA\text{-}AC}$ with

pXRCC4, indicating that this tight interaction is with the FHA domain of PNKP and is mediated by the phosphorylation of Thr-233 on XRCC4. In contrast, unphosphorylated XRCC4 bound PNKP-AC with a lower affinity ($K_d = 90 \pm 5$ nM) and had no significant effect on AC fluorescence when added to PNKP$^{FHA\text{-}AC}$, implying that XRCC4 binding is associated with the C-terminal catalytic kinase/phosphatase domain and not the FHA domain of PNKP. This was confirmed by the observation that XRCC4 quenched the AC fluorescence when mixed in 1:1 molar ratio with PNKP$^{CT\text{-}AC}$, yielding a K_d value of 100 ± 10 nM, in close agreement with the K_d value obtained with full-length PNKP. Far-UV CD measurements also demonstrated interaction between XRCC4 and PNKP^{CT}, because the experimentally observed CD spectrum for the XRCC4·PNKP^{CT} complex deviated from the theoretical CD spectrum.

The bimodal physical interaction of XRCC4 with PNKP observed here is similar to that of XRCC1; however, the effects of XRCC1 and XRCC4 on PNKP activity are dramatically different. In the case of XRCC1, both the CK2-phosphorylated and the nonphosphorylated protein stimulate PNKP kinase activity by enhancing PNKP dissociation from the phosphorylated substrate (19, 31–33). Furthermore, phosphorylation of XRCC1 elevates the stimulation of PNKP by XRCC1 (31, 32). This contrasts significantly with the pattern of activity displayed by XRCC4. Under circumstances designed to test for enzyme turnover, unphosphorylated XRCC4 was shown to stimulate PNKP kinase activity, whereas the CK2-phosphorylated protein not only failed to stimulate PNKP but actually inhibited PNKP kinase despite the formation of a ternary complex with PNKP and DNA. The interactions monitored by fluorescence clearly indicated that despite the presence of a large excess of DNA, pXRCC4 prevented the DNA from binding to PNKP within this complex. The PNKP-pXRCC4 interaction requires a region of pXRCC4 encompassing amino acid residues 213–250, whereas the DNA-binding region in XRCC4 is at the base of the head domain (spanning residues 1–200, with a requirement for residues 1–28 as well as residues 168–200) (3). Thus, the binding of DNA to pXRCC4 would be expected to maintain the DNA at a sufficient distance from PNKP-AC to prevent its interaction with the acrylodan dye. Both PNKP and pXRCC4 are capable of binding the DNA duplex with similar affinities ($K_d = \sim 0.5$ μM); hence the most likely explanation for the failure of PNKP to bind DNA in the tripartite complex is that binding to pXRCC4 physically occludes the DNA-binding sites (both kinase and phosphatase) of PNKP. Alternatively, binding of pXRCC4 to the FHA domain might cause a significant conformational change in PNKP that distorts the DNA-binding sites. We consider this possibility less likely because the linker region (residues 111–144) between the FHA domain and the catalytic domain is extremely flexible (15).

The effect of CK2-phosphorylated XRCC4 on PNKP activity was in sharp contrast to that of baculovirus expressed X4·LIV complex. Although XRCC4 in the context of the X4·LIV complex was phosphorylated on Thr-233, X4·LIV did not inhibit PNKP kinase activity. Thus, the inhibition of PNKP activity by pXRCC4 is suppressed when in the X4·LIV complex. We have yet to identify the reason for the altered behavior of pXRCC4 in this context. One possibility is that binding of the ligase to

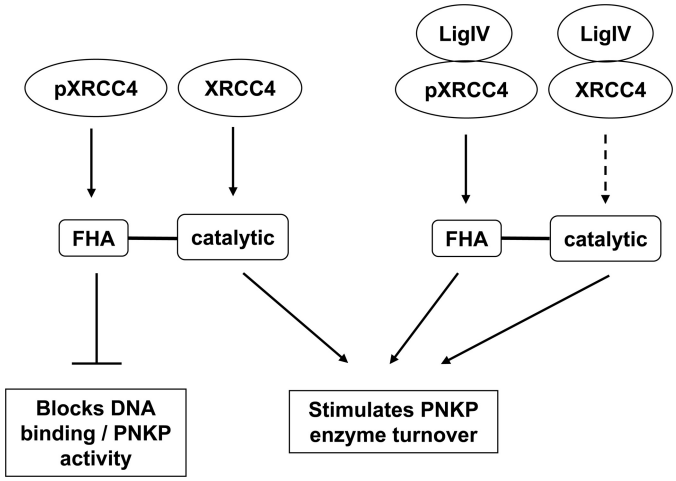

FIGURE 9. **Summary of effects of phospho-XRCC4 and non-phospho-XRCC4 on PNKP activity.**

pXRCC4 alters its interaction with DNA. In this regard, it is interesting to note that Drouet *et al.* (34) reported that the recruitment of XRCC4 to strand break termini is severely curtailed in the absence of DNA ligase IV. However, like bacterially expressed XRCC4, X4·LIV did stimulate PNKP enzyme turnover, and this was independent of Thr-233 phosphorylation status (Fig. 5).

XRCC4·PNKP Interactions within NHEJ—To date XRCC4 has been considered a scaffold protein that is recruited to and maintained at the site of damage by interaction with the Ku heterodimer (35, 36). DNA-PKcs subsequently stabilizes the recruited XRCC4 at DSBs. After this initial recruitment phase, the recruited proteins are thought to form large complexes by interacting with freely migrating unbound proteins, such as PNKP. Because of the tight binding of XRCC4 to DNA ligase IV, it has been argued that DNA ligase IV would be co-recruited with XRCC4 (36, 37). The discovery that phosphorylation of XRCC4 by CK2 gives rise to a high affinity interaction with the FHA domain of PNKP, and this interaction enhances ligation of radiation-induced DNA DSBs, further supported the scaffold/recruitment function of XRCC4 (7). However, the data presented here suggest that the involvement of XRCC4 in NHEJ is more complicated than previously thought. Specifically, we show that ~50% of XRCC4 in HeLa cells is phosphorylated on Thr-233. In addition, XRCC4 is present in molar excess over DNA ligase IV and PNKP. Together, these data suggest that not all of the cellular XRCC4 is in complex with DNA ligase IV, and because not all of the cellular XRCC4 is phosphorylated on Thr-233, approximately half of the XRCC4 would not be available for the high affinity FHA-mediated interaction with PNKP. We hypothesize that cells may contain multiple populations of XRCC4, some phosphorylated on Thr-233 and some not, some in complex with DNA ligase IV and some without, and that these proteins and protein complexes have subtly different effects on PNKP activity that may influence NHEJ and other repair pathways (summarized in Fig. 9). Our data suggest that one function for XRCC4 is the displacement of PNKP from processed strand break termini. This can be accomplished by nonphosphorylated XRCC4 alone or by phosphorylated or nonphosphorylated X4·LIV complex. A second likely role for

XRCC4 is the recruitment of DNA ligase IV to seal the breaks after PNKP processing of the termini. Such recruitment would presumably be enhanced by the tight binding between pXRCC4 and the FHA domain of PNKP and would explain the observation for phospho-dependent stimulation of DNA end joining by PNKP (7). Further experiments will be required to establish whether XRCC4 is essential for recruitment of PNKP to DSB termini in the cell.

Acknowledgment—We thank Dr. Reinhart Reithmeier (Department of Biochemistry, University of Toronto) for assistance with the sedimentation equilibrium measurements.

REFERENCES

1. Friedberg, E. C. W., Siede, G. C., Wood, R. D., Schultz, R. A., and Ellenberger, T. (2006) *DNA Repair and Mutagenesis*, ASM Press, Washington, D. C.
2. Mahaney, B. L., Meek, K., and Lees-Miller, S. P. (2009) *Biochem. J.* **417,** 639–650
3. Modesti, M., Hesse, J. E., and Gellert, M. (1999) *EMBO J.* **18,** 2008–2018
4. Li, Z., Otevrel, T., Gao, Y., Cheng, H. L., Seed, B., Stamato, T. D., Taccioli, G. E., and Alt, F. W. (1995) *Cell* **83,** 1079–1089
5. Grawunder, U., Zimmer, D., Kulesza, P., and Lieber, M. R. (1998) *J. Biol. Chem.* **273,** 24708–24714
6. Chappell, C., Hanakahi, L. A., Karimi-Busheri, F., Weinfeld, M., and West, S. C. (2002) *EMBO J.* **21,** 2827–2832
7. Koch, C. A., Agyei, R., Galicia, S., Metalnikov, P., O'Donnell, P., Starostine, A., Weinfeld, M., and Durocher, D. (2004) *EMBO J.* **23,** 3874–3885
8. Habraken, Y., and Verly, W. G. (1988) *Eur. J. Biochem.* **171,** 59–66
9. Jilani, A., Ramotar, D., Slack, C., Ong, C., Yang, X. M., Scherer, S. W., and Lasko, D. D. (1999) *J. Biol. Chem.* **274,** 24176–24186
10. Karimi-Busheri, F., Daly, G., Robins, P., Canas, B., Pappin, D. J., Sgouros, J., Miller, G. G., Fakhrai, H., Davis, E. M., Le Beau, M. M., and Weinfeld, M. (1999) *J. Biol. Chem.* **274,** 24187–24194
11. Pheiffer, B. H., and Zimmerman, S. B. (1982) *Biochem. Biophys. Res. Commun.* **109,** 1297–1302
12. Leber, R., Wise, T. W., Mizuta, R., and Meek, K. (1998) *J. Biol. Chem.* **273,** 1794–1801
13. Critchlow, S. E., Bowater, R. P., and Jackson, S. P. (1997) *Curr. Biol.* **7,** 588–598
14. Yu, Y., Wang, W., Ding, Q., Ye, R., Chen, D., Merkle, D., Schriemer, D., Meek, K., and Lees-Miller, S. P. (2003) *DNA Repair* **2,** 1239–1252
15. Bernstein, N. K., Williams, R. S., Rakovszky, M. L., Cui, D., Green, R., Karimi-Busheri, F., Mani, R. S., Galicia, S., Koch, C. A., Cass, C. E., Durocher, D., Weinfeld, M., and Glover, J. N. (2005) *Mol. Cell* **17,** 657–670
16. Nick McElhinny, S. A., Snowden, C. M., McCarville, J., and Ramsden, D. A. (2000) *Mol. Cell. Biol.* **20,** 2996–3003
17. Bosc, D. G., Graham, K. C., Saulnier, R. B., Zhang, C., Prober, D., Gietz, R. D., and Litchfield, D. W. (2000) *J. Biol. Chem.* **275,** 14295–14306
18. Mani, R. S., Karimi-Busheri, F., Fanta, M., Caldecott, K. W., Cass, C. E., and Weinfeld, M. (2004) *Biochemistry* **43,** 16505–16514
19. Mani, R. S., Fanta, M., Karimi-Busheri, F., Silver, E., Virgen, C. A., Caldecott, K. W., Cass, C. E., and Weinfeld, M. (2007) *J. Biol. Chem.* **282,** 28004–28013
20. Harlow, E. D., and Lane, D. (1988) *Antibodies: A Laboratory Manual*, pp. 521–523, Cold Spring Harbor Laboratory, Cold Spring Harbor, NY
21. van Gent, D. C., McBlane, J. F., Ramsden, D. A., Sadofsky, M. J., Hesse, J. E., and Gellert, M. (1995) *Cell* **81,** 925–934
22. Eastman, Q. M., Leu, T. M., and Schatz, D. G. (1996) *Nature* **380,** 85–88
23. Prendergast, F. G., Meyer, M., Carlson, G. L., Iida, S., and Potter, J. D. (1983) *J. Biol. Chem.* **258,** 7541–7544
24. Wu, P. Y., Frit, P., Meesala, S., Dauvillier, S., Modesti, M., Andres, S. N., Huang, Y., Sekiguchi, J., Calsou, P., Salles, B., and Junop, M. S. (2009) *Mol. Cell. Biol.* **29,** 3163–3172
25. Modesti, M., Junop, M. S., Ghirlando, R., van de Rakt, M., Gellert, M., Yang, W., and Kanaar, R. (2003) *J. Mol. Biol.* **334,** 215–228
26. Kim, D. H., Sarbassov, D. D., Ali, S. M., King, J. E., Latek, R. R., Erdjument-Bromage, H., Tempst, P., and Sabatini, D. M. (2002) *Cell* **110,** 163–175
27. Gatica, M., Jacob, G., Allende, C. C., and Allende, J. E. (1995) *Biochemistry* **34,** 122–127
28. Bernstein, N. K., Karimi-Busheri, F., Rasouli-Nia, A., Mani, R., Dianov, G., Glover, J. N., and Weinfeld, M. (2008) *Anticancer Agents Med. Chem.* **8,** 358–367
29. Wiederhold, L., Leppard, J. B., Kedar, P., Karimi-Busheri, F., Rasouli-Nia, A., Weinfeld, M., Tomkinson, A. E., Izumi, T., Prasad, R., Wilson, S. H., Mitra, S., and Hazra, T. K. (2004) *Mol. Cell* **15,** 209–220
30. Shen, J., Gilmore, E. C., Marshall, C. A., Haddadin, M., Reynolds, J. J., Eyaid, W., Bodell, A., Barry, B., Gleason, D., Allen, K., Ganesh, V. S., Chang, B. S., Grix, A., Hill, R. S., Topcu, M., Caldecott, K. W., Barkovich, A. J., and Walsh, C. A. (2010) *Nat. Genet.* **42,** 245–249
31. Loizou, J. I., El-Khamisy, S. F., Zlatanou, A., Moore, D. J., Chan, D. W., Qin, J., Sarno, S., Meggio, F., Pinna, L. A., and Caldecott, K. W. (2004) *Cell* **117,** 17–28
32. Lu, M., Mani, R. S., Karimi-Busheri, F., Fanta, M., Wang, H., Litchfeld, D. W., and Weinfeld, M. (2010) *Nucleic Acids Res.* **38,** 510–521
33. Whitehouse, C. J., Taylor, R. M., Thistlethwaite, A., Zhang, H., Karimi-Busheri, F., Lasko, D. D., Weinfeld, M., and Caldecott, K. W. (2001) *Cell* **104,** 107–117
34. Drouet, J., Delteil, C., Lefrançois, J., Concannon, P., Salles, B., and Calsou, P. (2005) *J. Biol. Chem.* **280,** 7060–7069
35. Yano, K., and Chen, D. J. (2008) *Cell Cycle* **7,** 1321–1325
36. Yano, K., Morotomi-Yano, K., Adachi, N., and Akiyama, H. (2009) *J. Radiat. Res.* **50,** 97–108
37. Chen, L., Trujillo, K., Sung, P., and Tomkinson, A. E. (2000) *J. Biol. Chem.* **275,** 26196–26205
38. Chen, Y. H., Yang, J. T., and Chau, K. H. (1974) *Biochemistry* **13,** 3350–3359